The crystallographic distribution of field-desorbed species*

J. A. Panitz

Sandia Laboratories, Albuquerque, New Mexico 87115
(Received 13 August 1973)

The complete crystallographic distribution of field-evaporated W^{3+} and W^{4+} as well as field-desorbed hydrogen has been observed by using a new technique called field desorption spectrometry. The distributions are obtained during a single evaporation event in a modified field-ion microscope by recording the desorption image displayed on a spherical CEMA detector time gated with the arrival of an ion species of preselected mass-to-charge ratio. Preliminary observations show no unique crystallographic origin for W^{3+} or W^{4+} at 78 or 27 K during field evaporation in vacuum or imaging gas. Hydrogen appears to originate at random insterstitial locations at the surface and is not uniquely associated with the protruding atoms imaged in a conventional ion micrograph. The general lack of a one-to-one correspondence between gated desorption and ion micrograph images suggests that using the atom probe to identify individual preselected ion micrograph image spots may be much more difficult than originally anticipated.

INTRODUCTION

The field-ion microscope[1] provides a simple but elegant means for observing a metal surface in atomic resolution. With the introduction of the atom probe[2] in 1967, the identity of individual surface species could be determined, providing a surface analytical device with single-atom resolution. Recently, a variation of the atom probe[3] has extended its capability to include single-atom identification at several different crystallographic locations during a single evaporation event in addition to permitting all imaged surface species to be identified at one time. In this paper we present a logical extension of this latter technique, yet one which departs completely from atom probe philosophy. Rather than attempt to determine the identity of a surface species producing a preselected ion-image spot, we wish to determine the complete crystallographic distribution of a surface species of preselected mass-to-charge ratio. The significant advantage of this approach is that one obtains the complete surface distribution of a given species during a single evaporation event and thereby avoids the surface altering and tedious procedure inherent in any statistically significant crystallographic distribution determination using the atom probe. We call this new technique field desorption spectrometry (FDS) and use it here to provide the first comprehensive crystallographic distribution data for the species present on the surface of clean tungsten.

THEORY

Surface species, field evaporated from the specimen as positive ions by a high-voltage pulse, enter the drift region of a time-of-flight spectrometer with energy

$$\tfrac{1}{2}mv^2 = qV_A = neV_A, \tag{1}$$

where m is the mass of any single ion, v is its velocity, q is its charge, e is the electronic charge, and V_A is a positive bias applied to the specimen.

After traveling a time T in the drift region of length d, given by

$$T = d/v, \tag{2}$$

the ions strike a curved Chevron CEMA detector,[4] providing a visible desorption image on its phosphor screen that can be photographically recorded. The travel time of a given ion species is obtained by combining Eqs. (1) and (2) to give

$$T = d[(m/n)(0.193V_A)^{-1}]^{\frac{1}{2}} \tag{3}$$

where T is in μsec, d is in meters, m/n is in amu, and V_A is in kV. Now suppose that instead of operating the CEMA continuously, it is turned on for a short time

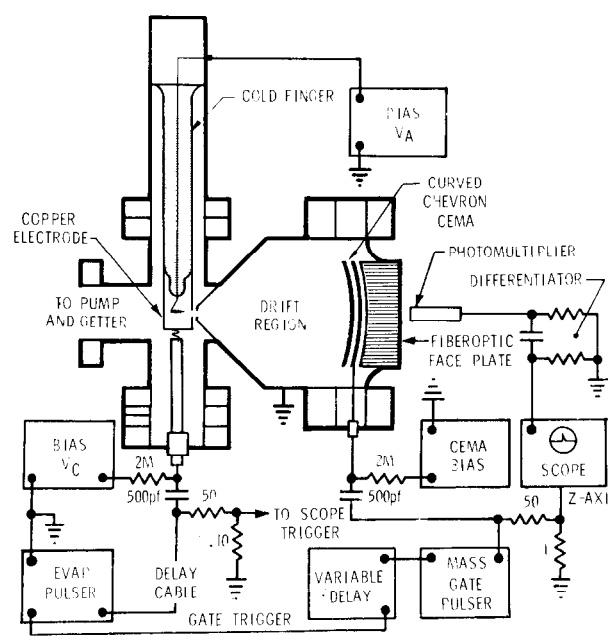

FIG. 1. Field desorption spectrometer. Desorbed surface species are detected by a time-gated curved Chevron CEMA detector so that only ions having a preselected mass-to-charge ratio will be displayed on its phosphor screen. This permits the complete crystallographic dependence of the given species to be recorded during a single evaporation event by placing photographic film (Polaroid Type 57) in contact with the CEMA's fiber-optic face plate. The delay cable from the evaporation pulser compensates for the inherent delay in the variable and mass gate pulsers.

coincidentally with the arrival of a preselected species of interest by applying a gate pulse a time T after the evaporation pulse has reached the specimen. If the duration of the gate pulse is shorter than the travel time between adjacent species, only that surface species having the unique travel time T will be detected and its complete crystallographic distribution displayed. Since individual ion impacts are resolved and recorded photographically, the number of recorded spots gives the absolute abundance of the detected species.[5]

APPARATUS

The apparatus is shown schematically in Fig. 1 and is identical to that described previously[3] except for the addition of the gating circuitry. During continuous operation of the CEMA (mass gate operative but not connected), the photomultiplier records the arrival of all ion species, and the resulting differentiated signal is displayed on an oscilloscope whose sweep is initiated by the evaporation pulse. A sample of this pulse is also displayed to provide a zero-time "fiducial" mark, and a sample of the gate pulse is used to modulate the oscilloscope sweep intensity so that the position of the mass gate relative to the ion peaks can be conveniently determined.

After selecting a species for investigation, the delay of the mass gate relative to the evaporation pulse is adjusted with the variable-delay generator until the intensified portion of the sweep coincides with the selected ion peak. The CEMA is then operated with the mass gate connected and the photomultiplier used to verify that the gated detector displays only the selected species. The optical coupling between the fiberoptics and the photomultiplier effectively isolates the sensitive photomultiplier circuitry from the fast high-voltage gate pulse.

FIG. 2. Helium ion image of the tungsten surface used in this study at 27 K and 6×10^{-7} Torr helium.

FIG. 3. Gated desorption image of W^{3+} at 78 K and 4×10^{-9} Torr during "gentle" evaporation. The complete crystallographic distribution of this species is displayed. Only the 110 region can be easily identified. Ion energy, 5.58 kV; $V_C=-5$ kV; $V_p=-1.5$ kV.

DETECTOR

During continuous operation, the curved CEMA is operated with 1 kV across each plate and 7 kV between the second plate and the screen. The front surface of the CEMA, which defines the end of the ion drift region, is usually held at ground potential.

To achieve gated operation, a positive pulse of 800 V is applied to the CEMA surface closest to the screen after reducing its dc potential to 1200 V.[6] Without applying the gate pulse, the CEMA gain is effectively zero, and no random noise images can be detected on Polaroid Type 57 film after a 30-sec exposure. Because only the ion species selected for examination is time correlated with the application of the narrow gate pulse, the signal-to-noise ratio of the detector is essentially infinite. This can be confirmed by moving the gate pulse in time to a position at which no ions were detected during nongated operation of the CEMA and exposing Type 57 film.

FIG. 4. Gated desorption image of W^{3+} at 78 K and 4×10^{-9} Torr during "severe" evaporation. The crystallographic distribution is essentially uniform. Ion energy, 5.58 kV; $V_C=-5$ kV; $V_p=-2.0$ kV.

In order to optimize both viewing and photographing of the gated image, a long-decay-time phosphor is desirable, but, since the arrival of the ions at the CEMA must be accurately determined by the photomultiplier, a short rise time is essential. These two diverse conditions are satisfied by settling equal parts of P1 and P47 phosphors on the fiberoptics viewing screen. The P1 phosphor provides a bright image for visual observation and photography, and the P47, matching the spectral response of the photomultiplier, provides the fast rise time which is required.

RESULTS AND CONCLUSIONS

Figure 2 shows a conventional helium ion image at 27 K of the tungsten surface used in this study. Since a desorption micrograph is always sharper than the corresponding ion micrograph, even at elevated temperatures,[7] much of our work has been done at 78 K.

Figure 3 is an example of mass gating for the dominant ion species W^{3+} and applying a desorption pulse to cause "gentle" field evaporation of the surface. Two features of this gated desorption micrograph are immediately obvious. First, W^{3+} does not appear to originate from specific crystallographic locations but appears to come from all areas of the surface with equal probability. Second, and perhaps more striking, is the general lack of a recognizable ion micrograph pattern. That is, there is not a unique one-to-one correspondence between the surface species imaged in the conventional ion micrograph and those recorded as a result of field evaporation. This does not appear to be due to CEMA characteristics as previously supposed[7] since there is obvious net plane symmetry in the 110 region that can be directly correlated with edge atoms imaged in the conventional ion micrograph. Rather, the disorder appears to be due to a statistical feature of the evaporation process, as well as local field variations (caused by local variations of the specimen's average radius of curvature) which cause locally different evaporation rates.[8] This is emphasized in Fig. 4, where W^{3+} was once again examined but at a much higher evaporation rate. The imaged area has in general begun to "fill in" while still preserving the identity of the 110 region. Since this region has the highest evaporation field of those imaged, the "filling in" of the micrograph is probably due to much more rapid evaporation in all other areas, which results in continual local removal of atoms from the specimen throughout a depth of perhaps several atomic layers.

Of particular interest are those atoms which appear to have field evaporated from the central area of the 110 plane or from the surrounding ledges, atoms which are

FIG. 5. Gated desorption image of W^{4+} at 78 K and 4×10^{-9} Torr. Ion energy, 2.5 V; $V_C=-6.25$ kV; $V_p=-1.3$ kV. The evaporation rate, as determined by monitoring W^{3+}, was severe since only under such conditions is the appearance of W^{4+} noticeable. The specimen is not the same one used to obtain Figs. 2–4 and 6.

not imaged in a conventional ion micrograph[9] and represent a very real manifestation of the statistical nature of the evaporation process. It is interesting to notice the converse at gentle evaporation rates (Fig. 3) where the statistical nature of the process is still evident. There, conventionally imaged atoms (edge atoms of the 110 plane) do not all field evaporate, as might be expected from *a priori* considerations.

As a result of the apparent statistical nature of the evaporation process, the ultimate aim of atom probe microscopy, "to determine the nature of one single atom seen on a metal surface and selected from neighboring atoms at the discretion of the observer,"[10] may be extremely difficult to achieve. This does not, however, detract from the more usual and practical use of the technique as an ultimate microanalytical capability for identifying the species present in a *small region* of the surface.

It is important to distinguish the lack of correlation between ion and gated desorption micrographs due to the statistical nature of the evaporation process or to local variations in evaporation rate from the lack of correlation due to a trajectory difference between the ionized imaging gas atom and the corresponding field-evaporated surface species.[11] In theory, one can compensate for this latter "aiming effect" in the atom probe by shifting the probe hole slightly away from the selected ion micrograph image spot[12] until a signal is recorded at the detector. In practice, however, the statistical nature of the evaporation process interferes since the detected signal may either represent the species originally intended for examination or a completely different species not originally imaged. Only by using a large probe hole several ion image spots in diameter to assure the detection of *something* can one eliminate this problem, but in doing so spatial resolution on the surface must be sacrificed.

If the instrument is gated for the less abundant species W^{4+} ($W^{4+} < 0.1W^{3+}$), one obtains the micrograph shown in Fig. 5. The most obvious feature of the W^{4+} micrograph when compared to those of W^{3+} is the lack of symmetry or indication of net plane structure in the 110 region. It is tempting to suggest that the production of W^{4+} is related, statistically, to W^{3+} production and one could produce a W^{4+} pattern by picking at random every tenth atom from a W^{3+} micrograph obtained during severe evaporation. In any event W^{4+}, which does not appear unless the evaporation rate is very large,[13] does not exhibit a strong crystallographic dependence but appears to be produced with essentially equal probability over the entire imaged surface.

Figure 6 is the result of gating for hydrogen adsorbed on the surface from residual hydrogen in the vacuum system. Since our resolution is not presently sufficient to separate mass 1 and 3, Fig. 4 may contain the desorption images of H_1^+, H_2^+, and H_3^+. Of particular interest is the lack of recognizable surface features. Since hydrogen was desorbed from the surface, the randomness of its pattern implies that it is adsorbed at interstitial locations on the surface and does not preferentially associate with the protruding atoms imaged in a conventional ion micrograph. There is a suggestion from Fig. 5 when compared with the ion micrograph image of Fig. 3 (and enforced by repeated desorption observations) that the 110 region contains less adsorbed hydrogen than the regions closer to the tip shank. This may be reasonable since migration from the shank would be expected to at least partially replenish the surface coverage between evaporation pulses.

FIG. 6. Gated desorption image of residual hydrogen field desorbed from the tungsten emitter shown in Fig. 1 at 78 K and 6×10^{-9} Torr. The lack of symmetry, particularly in the 110 region, suggests that hydrogen is field desorbed from random interstitial locations on the surface. Ion energy, 4.0 kV; $V_C = -5.5$ kV; $V_p = -1.5$ kV.

ACKNOWLEDGMENTS

The author wishes to thank J. Abraham of the Bendix Corp. who manufactured the curved CEMA plates in an elegantly simple manner, V. Nogle for his technical assistance, and R. Snidow and F. Tenant for their cooperation and glass-working expertise.

*Supported by the U. S. Atomic Energy Commission.

[1] E. W. Müller and T. T. Tsong, in *Field Ion Microscopy, Principles and Applications* (Elsevier, New York, 1969).
[2] E. W. Müller and J. A. Panitz, 14th Field Emission Symposium, National Bureau of Standards, Washington, D. C., (unpublished).
[3] J. A. Panitz, Rev. Sci. Instrum. **44**, 1034 (1973).
[4] Manufactured by The Bendix Corp., Electro-Optics Division, Galileo Park, Sturbridge, Mass. The specimen is placed at the

center of curvature of the CEMA to ensure identical travel times for all ion species.

[5]The absolute abundance of the detected species on the surface *prior* to field evaporation can be determined from these data only if the entire surface layer of atoms has been removed and if the active area of the CEMA is sufficiently large to assure detection of essentially all ions striking it.

[6]The width of the gate pulse essentially determines the mass resolution, since it provides a "time window" during which the CEMA has gain. At its maximum amplitude of 800 V the gate pulse is 10 nsec wide, and its width increases to 30 nsec at 200 V. At this point the total potential (dc bias +pulse amplitude) is 1000 V, and the resulting CEMA gain is insufficient to detect desorbed species.

[7]A desorption microscope using a single channel plate and external image intensifier was described by R. J. Walko and E. W. Müller, Phys. Status Solidi A **9**, K9 (1972). Mass analysis of the detected species was not possible.

[8]An alternate explanation is that a surface species, immediately prior to removal from the surface as a positive ion, exists in a metastable state whose surface location does not coincide with the species' original surface position. Subsequent removal from this new surface position would lead to a detected image lacking correspondence with a conventional ion image. However, this mechanism does not appear to be too probable in view of the 110 region symmetry unless its importance is dependent on specific crystallographic location.

[9]Another possibility is that such images represent conventionally imaged surface atoms whose trajections during field evaporation are significantly but randomly altered from those of neighboring species. Since the probability of appearance of the "misplaced" atoms seems to increase directly with the severity of the evaporation event, it is usually desirable to minimize the evaporation rate consistent with the ability to remove species of interest.

[10]E. W. Müller, J. A. Panitz, and S. B. McLane, Rev. Sci. Instrum. **39**, 83 (1968).

[11]E. W. Müller, 15th Field Emission Symposium, Bonn, Germany 1968 (unpublished); J. A. Panitz, Ph.D. dissertation, The Pennsylvania State University, 1969.

[12]E. W. Müller, Ber. Bunsenges. **75**, 979 (1971).

[13]It is not obvious whether the production of W^{4+} is due to a large evaporation rate or to the correspondingly large evaporation field. That is, it is difficult to determine if the production mechanism is rate or field-dependent.